

Hydrogel for Simultaneous Tunable Growth Factor Delivery and Enhanced Viability of Encapsulated Cells *in Vitro*

James Parker,^{†,‡,⊥} Nikolaos Mitrousis,^{‡,§,⊥} and Molly S. Shoichet^{*,†,‡,§,||}

[†]Department of Chemistry, University of Toronto, 80 St. George Street, Toronto, Ontario M5S 3H6, Canada

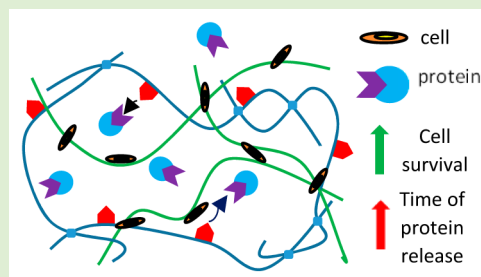
[‡]Donnelly Centre, University of Toronto, 160 College Street, Toronto, Ontario M5S 3E1, Canada

[§]Institute of Biomaterials and Biomedical Engineering, University of Toronto, 164 College Street, Toronto, Ontario M5S 3G9, Canada

^{||}Department of Chemical Engineering and Applied Chemistry, University of Toronto, 200 College Street, Toronto, Ontario M5S 3E1, Canada

S Supporting Information

ABSTRACT: Poor cell survival *in vitro* and *in vivo* is one of the key challenges in tissue engineering. Prosurvival therapeutic proteins, such as insulin-like growth factor-1 (IGF-1), can promote cell viability but require controlled delivery systems due to their short half-lives and rapid clearance. Biocompatible materials are commonly used for drug delivery platforms or to encapsulate cells for increased viability, but few materials have been used for both applications simultaneously. In this work, we present a dual-use platform. A blend of hyaluronan and methylcellulose, known to promote cell survival, was covalently modified with Src homology 3 (SH3)-binding peptides and demonstrated tunable, affinity-based release of the prosurvival fusion protein SH3-IGF-1. The material also significantly increased the viability of retinal pigment epithelium cells under anchorage-independent conditions. This novel platform is applicable to a broad range of cells and protein therapeutics and is a promising drug delivery/cell transplantation strategy to increase the viability of both exogenous and endogenous cells in tissue engineering applications.



1. INTRODUCTION

Increasing cell viability both *in vitro* and *in vivo* is a major challenge in regenerative medicine. Poor survival rates are characteristic of both endogenous cells damaged by degenerative diseases and the exogenous cells used to replace them. Protein therapeutics are an effective method to improve cell viability, but many proteins suffer from short half-lives *in vitro* and *in vivo* and are cleared quickly from the body, limiting their efficacy.^{1,2}

Implantable drug delivery systems made from a variety of materials are commonly used to prolong the effects of protein therapeutics.^{3–6} This is preferably achieved with materials that provide tunable release of the therapeutic in order to maximize its efficacy and applicability.⁷ A common strategy is the use of nano- or microparticles embedded in a polymer matrix to provide a diffusive barrier that attenuates protein release.^{8–11} However, these particle-based systems often suffer from poor protein loading and denaturation during processing.^{12,13} Affinity release systems overcome these limitations by avoiding the use of harsh chemicals;⁷ instead, they take advantage of the interaction between the growth factors and matrix to attenuate release, as has been shown with hyaluronan,^{14,15} heparin–poly(lactic-co-glycolic acid) (PLGA),¹⁶ and alginate,¹⁷ among others.

Cell transplantation has emerged as a compelling therapeutic approach for neurodegenerative diseases that are currently incurable.¹⁸ One of the most promising targets for such regenerative therapies is the eye due to its immunoprivileged nature and the clearly defined transplantation site.^{19–21} Retinal pigment epithelium cells (RPE) are found at the posterior of the retina, and their death and dysfunction are associated with many degenerative diseases, including age-related macular degeneration (AMD), the most common form of irreversible blindness in the developed world.^{21–24} Transplantation of new RPE cells to reverse AMD is currently being pursued in clinical trials.²⁵ Despite significant progress in the field, the efficacy of cell transplantation is still hindered by low cell survival, improper distribution, and minimal integration into the host tissue.¹⁸ In the vast majority of studies, cell survival after transplantation into the eye is in the range of 1–2%.¹⁸ In addition, many of the surviving cells do not adopt the proper tissue morphology and instead form multicellular aggregates that prevent their integration into the functional circuitry of the eye. We have shown that a hydrogel comprising hyaluronan and methylcellulose (HAMC) can greatly increase the survival and

Received: October 9, 2015

Revised: January 8, 2016

Published: January 13, 2016

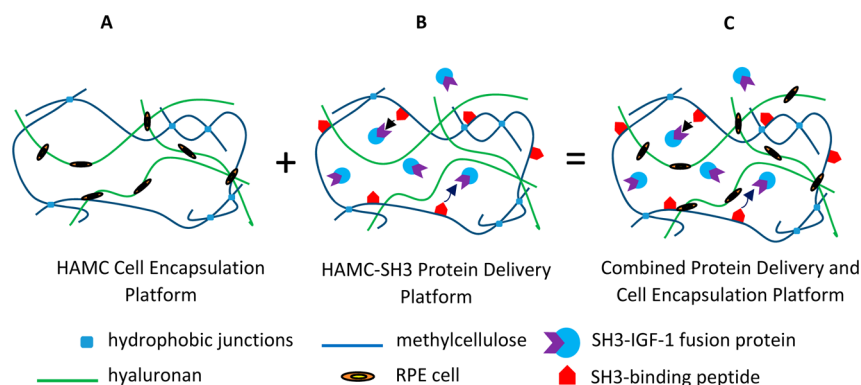


Figure 1. Schematic of hydrogel designed for combined tunable affinity release of protein therapeutics and cell encapsulation. (A) Hyaluronan and methylcellulose hydrogel (HAMC) known to increase cell viability; (B) modified HAMC with SH3-binding peptide for the affinity release of SH3–IGF-1 fusion protein; (C) modified HAMC hydrogel with encapsulated cells.

integration of retinal stem cell-derived rod photoreceptor progenitors into the host eye.^{25,26} RPE cells suffer from poor survival on nonadhesive environments *in vitro* and *in vivo*,^{24,26,27} such as those found immediately after scaffold-free cell transplantation. Increasing the survival of RPE in both *in vitro* and *in vivo* environments is one of the major challenges of current RPE treatments.²⁷

Materials comparable or identical to those used in these drug delivery systems can also be used to encapsulate cells and improve their viability through cell interactions with covalently attached growth factors or the material itself.^{28–31} However, despite the use of similar or identical materials in both drug delivery and pro-survival cell encapsulation platforms, few materials have been designed for simultaneous use in both applications. Such a material could potentially be used to simultaneously improve the effects of protein therapeutics, through sustained delivery, and the viability of encapsulated cells via interactions with the biomaterial and localized drug.³²

HAMC is biocompatible, fast-gelling, and injectable,^{33,34} and it promotes wound healing and reduces inflammation.³⁵ It has been shown to increase transplanted cell survival in the retina, brain, and spinal cord^{31,36,37} and can be modified to allow the sustained delivery of protein therapeutics.^{7,14} It is an excellent candidate for use as a dual drug delivery and pro-survival cell delivery material for RPE.

The choice of protein therapeutic for delivery is equally as important as that of the cell type. A factor with strong trophic effects on RPE as well as broad applicability to a wide variety of cell types would be ideal. Insulin-like growth factor-1 (IGF-1) is a potent therapeutic, which enhances the viability of many cell types^{38–45} and has been shown to improve the survival, proliferation, and migration of RPE *in vitro* and *in vivo*.^{46–51} There is also strong indirect evidence that IGF-1 reduces RPE apoptosis under anchorage-independent conditions, such as those found in advanced retinal degeneration.^{52–59} Tunable release of IGF-1⁶⁰ is required to maximize its efficacy in a broad range of applications, including cartilage growth,^{38,61,62} cardioprotection,³⁹ and retinal cell proliferation and survival.^{51,63}

Here, we present a HAMC hydrogel (Figure 1) that has been covalently modified to provide tunable affinity release of IGF-1 while simultaneously increasing the viability of encapsulated RPE under nonadhesive conditions *in vitro*.

2. EXPERIMENTAL SECTION

2.1. Materials. 3-Maleimidopropionic acid was purchased from TCI America (Portland, USA). Modified pET32b vector was a gift from Dr. Karen Maxwell (University of Toronto). Cloning of the SH3-FGF-2 and IGF-1 vectors was done by GenScript (Piscataway, USA). Sodium hyaluronate (1.4×10^6 to 1.8×10^6 g/mol) was purchased from Kikkoman Biochemifa (Tokyo, Japan). Methyl cellulose (3×10^5 g/mol) was purchased from Shin Etsu (Tokyo, Japan). Sandwich ELISA kit for human IGF-1 was purchased from Assaypro (St. Charles, USA). All buffers were made with distilled and deionized water prepared using a Millipore Milli-RO 10 plus and Milli-Q UF Plus at 18 M Ω resistance (Millipore, Bedford, USA). Artificial cerebrospinal fluid (aCSF) was prepared as previously described.⁶⁴ All other solvents and reagents were purchased from Sigma-Aldrich and used as received. Human embryonic stem cells were supplied from Dr. Andras Nagy (University of Toronto).

2.2. Methods. **2.2.1. Synthesis of SH3–IGF-1 Gene.** The IGF-1 gene was amplified from the IGF-1 gene (Genscript) by PCR using the forward primer CTGGCGGTGCACCGATGGCCGGCCCCGAAAC and the reverse primer GTGCGGCCGCAAGCTTTTATCAGGCCGATTTCGCCGG. The SH3-linker gene was amplified from the SH3-FGF-2 gene using the forward primer TTCCAGGCGCC-ATGGCCCCGTGGGCTACCGCA and the reverse primer TTCCGGGCCGGCCATCGGTGCACCGCCAGAG. Both genes were purified using QiaGen PCR purification kit and combined into the SH3–IGF-1 gene by PCR using the IGF-1 forward primer and the SH3 reverse primer. The SH3–IGF-1 gene and modified pET32b plasmid were digested with NcoI-HF and HindIII-HF, purified with QiaGen PCR purification kit, and ligated using Clontech InFusion kit. The resulting vector was used to transform chemically competent *E. coli* BL21.

2.2.2. Expression and Purification of SH3–IGF-1. *E. coli* BL21 colonies were selected and grown in 20 mL of LB with 100 μ g/mL ampicillin for 18 h and used to inoculate large cultures in 1.8 L LB flasks containing 100 μ g/mL and 10 drops of Anti-Foam 204. The large cultures were grown with air sparging at 37 °C until OD₆₀₀ = 0.8. Expression was induced using a final concentration of 0.8 mM IPTG and maintained for 24 h at 16 °C. The cultures were centrifuged at 7000 rpm (Beckman Coulter centrifuge Avanti J-6 with rotor JLA-8.1000) for 10 min and resuspended in 20 mL of 6 M guanidine hydrochloride, 0.1 M NaH₂PO₄, 10 mM Tris, 10 mM imidazole, pH 8.0 (Buffer A). The resuspended pellets were incubated on a rotator at 4 °C for 16 h and centrifuged at 45 000g (Beckman Coulter centrifuge Avanti J-26 with rotor JA-25.50) for 15 min, and the supernatant was collected. The supernatant was incubated with 2 mL of Ni-NTA agarose for 25 min and washed five times with 20 mL of Buffer A. The protein was eluted by adding 50 mL of 6 M guanidine hydrochloride containing 0.2 M acetic acid.

Purified SH3–IGF-1 was refolded by dialyzing (8 kDa MWCO) in 50 mM Tris, 125 mM arginine, 5 mM cysteine for 36 h at 4 °C. The

protein was then dialyzed against 50 mM Tris, 0.5 mM EDTA, pH 8.0 (tobacco etch virus protease (TEV) cleavage buffer), for 36 h and concentrated to 0.2–0.3 mg/mL. Three millimolar glutathione (reduced), 0.3 mM glutathione (oxidized), and TEV at a 6:100 TEV/SH3–IGF-1 ratio were added, and the mixture was incubated for 24 h at room temperature to cleave the thioredoxin (Trx) domain. The resulting mixture was incubated for 30 min with 2 mL of Ni-NTA and filtered through a gravity filtration column. The eluent was collected, passed through again, and collected as pure SH3–IGF-1. Pure SH3–IGF-1 was dialyzed (3.5 kDa MWCO) against 50 mM Tris, 100 mM NaCl, pH 8.0, buffer for 48 h, sterile-filtered, and stored at -80°C for future use.

2.2.3. SH3–IGF-1 Bioactivity. Two million MCF-7 cells were seeded on a T-25 flask and grown for 24 h in DMEM/F-12 with 10% FBS, 1% penicillin/streptomycin (P/S), and 1% insulin. Cells were trypsinized, and 2×10^4 cells/mL (200 μL) were added per well in a 96-well plate and allowed to attach at 37°C for 24 h. The cells were serum-starved for 24 h, after which the media was replaced with either serum-free media, serum-free media with 50 ng/mL commercial IGF-1, or serum-free media with 50 ng/mL recombinant SH3–IGF-1. The cells were cultured for 48 h, and proliferation was determined by CellTiter 96 AQueous One Solution Cell Proliferation (MTS) assay (Promega).

2.2.4. Preparation of MC Modified with SH3-Binding Peptide. MC was covalently modified with SH3-binding peptide (either weak-binding peptide (WBP) GGGKPPVVKKPHYLS, $K_D = 2.7 \times 10^{-5}$ M, or strong-binding peptide (SBP) GGGKTKPTPPKPSHLKPK, $K_D = 2.7 \times 10^{-7}$ M) as described previously.⁷ Briefly, carboxylated MC was prepared using a Williamson ether synthesis and converted to thiolated MC (MC-SH) by coupling with 3,3'-dithiobis(propionic dihydrazide) (DTP) via 1-ethyl-3-[3-(dimethylamino)propyl]-carbodiimide (EDC) and reducing with dithiothreitol (DTT). Michael addition was then used to couple the MC-SH to maleimide-WBP or maleimide-SBP. A schematic of the reactions is shown in Figure 2.

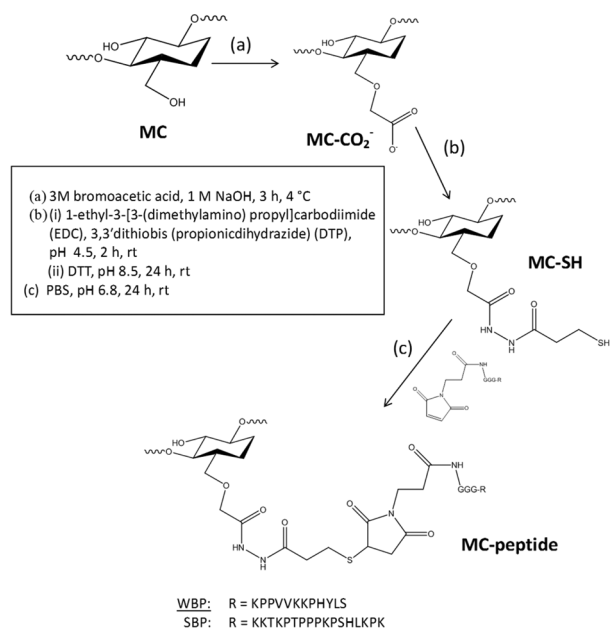


Figure 2. Schematic for the preparation of MC-peptide from unmodified MC.

2.2.5. In Vitro SH3–IGF-1 Release from HAMC, HAMC-SBP, and HAMC-WBP. HAMC and HAMC-peptide hydrogels were prepared by adding 310 $\mu\text{g}/\text{mL}$ SH3–IGF-1 (46.8 μL , 890 pmol) and sterile-filtered aCSF (46.8 μL) to (i) 1.4 mg of HA and 5 mg of MC (HAMC gel); (ii) 1.4 mg of HA, 2.91 mg of MC, and 2.09 mg MC-WBP (115 nmol WBP/mg MC, WBP/SH3–IGF-1 = 270:1, HAMC-WBP gel); or (iii) 1.4 mg of HA, 4.49 mg of MC, and 0.51 mg of MC-SBP (88

nmol SBP/mg MC, SBP/SH3–IGF-1 = 50:1, HAMC-SBP gel) in sterile 2 mL Eppendorf tubes. The samples were dispersed using a planetary mixer, centrifuged at 16 162g (Sigma 1-14 microcentrifuge) to remove air bubbles, and dissolved overnight at 4°C . Samples were gelled by incubation on an orbital shaker at 37°C for 7 min, and 900 μL of sterile 37°C aCSF was added to simulate *in vivo* dilution conditions. At the specified time points (1, 3, 5, 8, 24, 48, 96, 168, 240 h), the aCSF was removed and replaced. Aliquots were frozen at -20°C until used in a sandwich ELISA (Assaypro, human IGF-1 ELISA kit) to determine SH3–IGF-1 concentration. The standard curve in the ELISA was prepared using serial dilutions of the expressed SH3–IGF1.

2.2.6. Gel Degradation Study. HAMC hydrogels were prepared by adding sterile-filtered aCSF (115 μL) to (i) 1.72 mg of HA and 6.14 mg of MC (HAMC gel); (ii) 1.72 mg of HA, 3.57 mg of MC, and 2.57 mg MC-WBP (115 nmol WBP/mg MC, HAMC-WBP gel); or (iii) 1.72 mg of HA, 5.51 mg of MC, and 0.63 mg of MC-SBP (88 nmol SBP/mg MC, HAMC-SBP gel) in sterile 2 mL Eppendorf tubes. The Eppendorf tubes were weighed individually before the beginning of the experiment. The samples were dispersed using a planetary mixer, centrifuged at 16 162g (Sigma 1-14 microcentrifuge) to remove air bubbles, and dissolved overnight at 4°C . Samples were gelled by incubation on an orbital shaker at 37°C for 7 min, and 1105 μL of sterile 37°C aCSF was added to simulate *in vivo* dilution conditions. The aCSF was removed immediately, and the gel-containing tubes were weighed, which constituted the t_0 weight. The aCSF was then replenished, and the samples were incubated at 37°C on an orbital shaker. At the specified time points (1, 3, 5, 8, 24, 48, 96, 168, 240, 336 h), the aCSF was removed, the samples were weighed, and the aCSF was replaced.

2.2.7. Effects of HAMC-SBP and HAMC-WBP with SH3–IGF-1 on RPE Survival and Proliferation in Vitro. 96-well plates were coated with poly(2-hydroxyethyl methacrylate) (poly(HEMA)) as described by Phung et al.⁶⁵ 60 μL of poly(HEMA) in 95% ethanol (5 mg/mL) was added to each well of a 96-well plate under sterile conditions. The plates were incubated at room temperature for 96 h with the lids on and 1 h with the lids off, sealed with parafilm, and stored at 4°C for 24 h before using.

RPE were derived from human embryonic stem cells as shown previously.⁶⁶ CA1 human embryonic stem cells were cultured on Geltrex (Life Technologies) in mTESR medium (Stem Cell Technologies). For differentiation, cells were grown to confluence (12–14 days post plating), and the medium was then changed to DMEM/F-12 containing 13% knockout serum replacement, 1% nonessential amino acids, 1% Glutamax, 1% penicillin/streptomycin, and 0.1% β -mercaptoethanol (all from Life Technologies). The cells were fed every other day, and pigmented clusters started appearing 3–4 weeks after the beginning of differentiation. The clusters were allowed to enlarge for another 4 weeks (in total, 7–8 weeks of differentiation) and were then manually picked using a scalpel under a dissection microscope. The picked colonies were dissociated with 0.25% trypsin and plated on Geltrex in full media, consisting of DMEM/F-12 containing 7% knockout serum replacement, 5% Hyclone FBS (Thermo Scientific), 1% nonessential amino acids, 1% Glutamax, 1% penicillin/streptomycin, 0.1% β -mercaptoethanol, and 10 ng/mL basic fibroblast growth factor (R&D Systems). After allowing the picked cells to grow for 2 weeks, the centers of the colonies, which exhibited uniform cobblestone morphology, were repicked using the same method. These double-picked cells formed monolayers with cobblestone morphology and uniformly expressed RPE markers at the protein and RNA levels. For immunostaining, the following antibodies were used: anti-RPE65 (Novus Biologicals, 1:200), anti-Bestrophin (Novus Biologicals, 1:200), and anti-ZO-1 (Life Technologies, 1:100).

HAMC gels (0.9% HA/0.9% MC (w/v)) were made in 1.25 mL bulk gels of HAMC alone (11.25 mg of HA and 11.25 mg of MC), HAMC-WBP (11.25 mg of HA, 8.25 mg of MC, and 3 mg of MC-WBP), or MC-SBP (11.25 mg of HA, 10.13 mg of MC, and 1.12 mg of MC-SBP) by adding 614 μL of serum-free DMEM/F-12 and 614 μL of 50 mM Tris, 100 mM NaCl, pH 8 (HAMC gels) or 614 μL of 53.4

$\mu\text{g/mL}$ SH3–IGF-1 in 50 mM Tris, 100 mM NaCl, pH 8 (HAMC-WBP and HAMC-SBP gels). The samples were dispersed using a planetary mixer, centrifuged at 16 162g (Sigma 1-14 microcentrifuge) to remove air bubbles, and dissolved overnight at 4 °C. RPE cells (1.6×10^5 cells/mL) were diluted 1:6 in serum-free DMEM/F-12, DMEM/F-12 + 10% FBS, or the appropriate 0.9% HA/0.9% (w/v) HAMC gel (final composition 0.75% HA/0.75% MC w/v). The cells in were plated on the poly(HEMA)-coated plates at 75 μL per well and incubated for 10 min at 37 °C to allow gels to form. Serum-free media (125 μL) was then added (final cell concentration of 1×10^4 cells/mL). Prestoblu fluorescence was used to measure RPE viability at 0, 48, and 96 h.

2.2.8. Statistical Analysis. Statistical analysis was done in Graphpad Prism, version 5. Unpaired Student's *t* test was used to compare two groups, and one-way ANOVA with Tukey's *post hoc* test was used to compare multiple groups. Graphs are annotated with *p* values represented as **p* \leq 0.05, ***p* \leq 0.01, and ****p* \leq 0.001.

3. RESULTS AND DISCUSSION

The SH3-linker gene (228 base pairs (bp)) and IGF-1 gene (216 bp) were PCR-amplified from their source vectors and ligated together to create the SH3–IGF-1 gene (444 bp) as detected by agarose gel electrophoresis (Supporting Information Figure S1). The gene was successfully ligated into the pET32b plasmid, which appends a thioredoxin (Trx) sequence to the N-terminus to aid with protein refolding and solubilization, and transformed into *E. coli* BL21. Trx–SH3–IGF-1 was expressed at high levels in BL21 *E. coli* and successfully purified (Supporting Information Figure S1B), after which the Trx domain was cleaved by TEV protease and removed using Ni-NTA chromatography (Supporting Information Figure S1C). The mass of the final product was confirmed by mass spectrometry (Supporting Information Figure S2).

To verify the bioactivity of our SH3–IGF-1, we compared it to commercially available IGF-1 in terms of MCF-7 cell proliferation.^{67,68} SH3–IGF-1 was found to stimulate MCF-7 proliferation to the same degree as commercially available IGF-1, as determined by the MTS metabolic assay after 48 h (Figure 3). There was a significant difference (*p* < 0.001) in the number

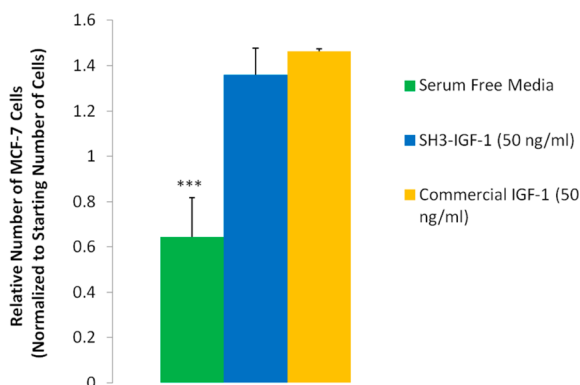


Figure 3. SH3–IGF-1 has equivalent bioactivity to that of commercially available IGF-1. MCF-7 cells were cultured on 96-well plates in DMEM/F-12 with 10% FBS and 1% P/S for 24 h and then serum-starved for 24 h. The cells were incubated in serum-free media containing SH3–IGF-1 (50 ng/mL) or commercial IGF-1 (50 ng/mL) for 48 h. Proliferation was measured using an MTS colorimetric assay. Both SH3–IGF-1 and commercial IGF-1 caused significantly different proliferation from that of the control, but they were not significantly different from each other (*n* = 3; mean \pm standard deviation plotted; *** indicates *p* < 0.001, ANOVA, Tukey's *post hoc* test).

of live cells between serum-free conditions and both commercially available IGF-1 and SH3–IGF-1. There was no significant difference (*p* > 0.05) in the formazan absorbance signal between cells treated with commercial IGF-1 and SH3–IGF-1.

In order to investigate affinity release of SH3–IGF-1, maleimide-conjugated SH3-binding peptides were successfully bound to thiolated MC via Michael addition. Two binding peptides were immobilized: either weak-binding peptide (WBP) GGGKPPVVKKPHYLS, $K_D = 2.7 \times 10^{-5}$ M, or strong-binding peptide (SBP) GGGKTKPTPPKPSHLKPK, $K_D = 2.7 \times 10^{-7}$ M. By amino acid analysis, substitution was determined to be, on average, 130 nmol for WBP/mg MC and 89 nmol for SBP/mg MC with no detectable protein adsorption on dialysis controls of maleimide-peptide with nonthiolated MC.

The release of SH3–IGF-1 from HAMC, HAMC-WBP, or HAMC-SBP was compared. After 24 h, approximately 67% of SH3–IGF-1 was released from HAMC, 40%, from HAMC-WBP, and 19%, from HAMC-SBP (Figure 4A). HAMC and HAMC-WBP released SH3–IGF-1 for 4 and 10 days, respectively, whereas HAMC-SBP gels appeared to stop releasing SH3–IGF-1 after 24 h, with only nanogram quantities of SH3–IGF-1 (0.03% of total) released over subsequent time points.

To ensure that the release profile was indeed due to the reversible binding of SH3 with its weak and strong binding partners and not due to changes in degradation profiles, the mass of the gels was measured over the same time frame as that followed for release. We observed no significant change in the degradation profiles of HAMC vs HAMC-WBP and HAMC-SBP (Figure 4B), thereby confirming the reversible binding with SH3 and its binding partners as the mechanism for the different release profiles.

The rates of SH3–IGF-1 release from HAMC, HAMC-WBP, and HAMC-SBP were significantly different. Release rates were compared using a plot of cumulative fractional protein release against the square root of time (Figure 5). This was done by assuming unidirectional diffusion from a plane sheet, as has been previously done for this affinity system,^{7,14} using the equation

$$\frac{M_t}{M_\infty} = kt^{1/2}$$

where M_t is the mass of drug released at time *t*, M_∞ is the mass of drug released as time approaches infinity, and *k* is the diffusion constant and slope of the line in the graph. The linear fit of the data is indicative of Fickian diffusion (Figure 5A), and the slopes of the curves are proportional to the protein diffusivity within the gel.⁶⁹ All *k* values were significantly different among HAMC ($k = 2.59 \times 10^{-3}$), HAMC-WBP ($k = 1.35 \times 10^{-3}$), and HAMC-SBP ($k = 7.92 \times 10^{-3}$) (*p* < 0.001 between HAMC and HAMC-WBP or HAMC-SBP; *p* < 0.001 between HAMC-WBP and HAMC-SBP) (Figure 5B). HAMC and HAMC-SBP showed Fickian diffusion release (applicable for the first 60% of protein release) for the first 8 h, whereas HAMC-WBP showed extended Fickian diffusion to 48 h. (Note that these values are expressed as the square root of time in seconds in Figure 5.)

Interestingly, HAMC-WBP gels were able to release up to 25% more IGF-1 than a similar, nontunable IGF-1 affinity release system over a similar time scale.⁶² Notably, comparable

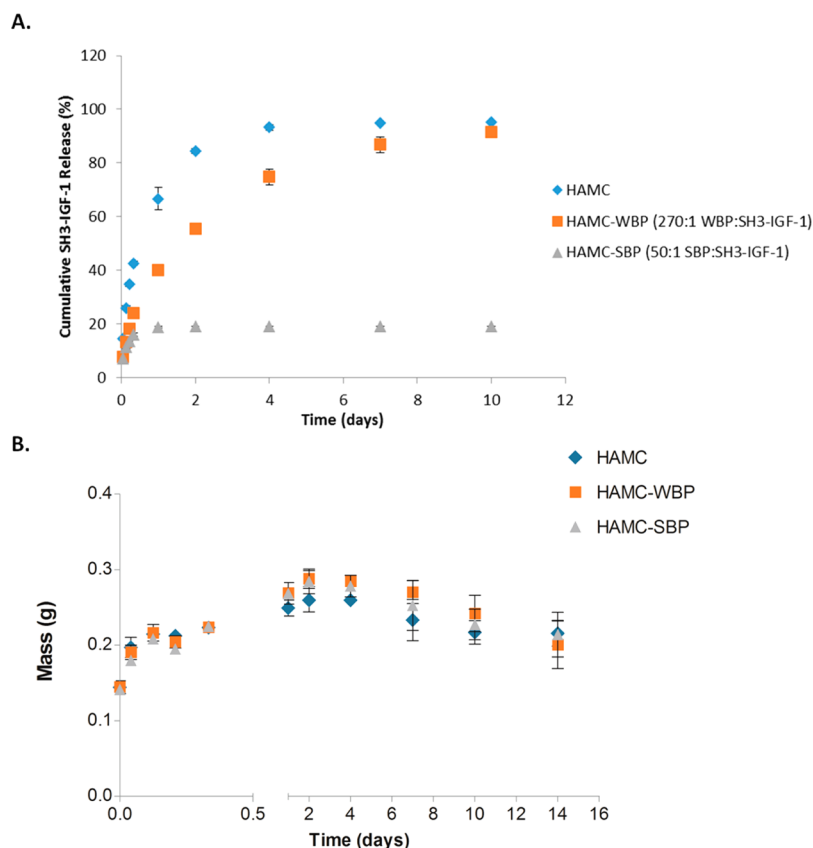


Figure 4. (A) *In vitro* cumulative release profile of SH3–IGF-1 delivered from HAMC, HAMC-weak binding peptide hydrogels (HAMC-WBP, 270:1 molar ratio of WBP/SH3–IGF-1), and HAMC-strong binding peptide (HAMC-SBP, 50:1 molar ratio of SBP/SH3–IGF-1). SH3-binding peptides attenuate release such that different release profiles are achieved ($n = 3$; mean \pm standard deviation plotted). (B) To ensure that the release profile is unaffected by degradation, the mass loss of HAMC vs HAMC-WBP and HAMC-SBP was compared: conjugation of these SH3-binding peptides to MC did not alter the degradation profile of the HAMC gels ($n = 3$; mean \pm standard deviation plotted; $p > 0.05$, ANOVA, Tukey's *post hoc* test).

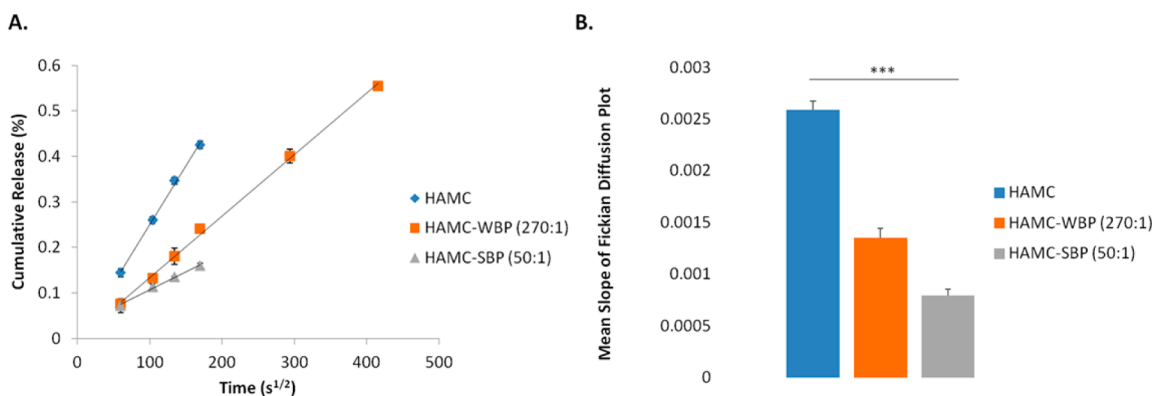


Figure 5. Cumulative release of SH3–IGF-1 from HAMC, HAMC-WBP (270:1 molar ratio WBP/SH3–IGF-1), and HAMC-SBP (50:1 molar ratio SBP/SH3–IGF-1) against the square root of time. (A) The slope of SH3–IGF-1 release from HAMC, HAMC-WBP, and HAMC-SBP hydrogels against the square root of time. The slope is representative of Fickian diffusion coefficient, k , for each gel. (B) Graphical representation of the slopes of SH3–IGF-1 release from each hydrogel and with significance indicated (** $p < 0.01$ and *** $p < 0.001$, ANOVA, Tukey's *post hoc* test; $n = 3$; mean \pm standard deviation plotted).

amounts of total protein were released from the HAMC and HAMC-WBP systems, an effect that is not commonly seen in affinity release systems as slower releasing platforms often release lower amounts of detectable protein.^{14,62,70–72}

The plateau in release from HAMC-SBP gels had not been previously observed at this early time point with this system.^{7,14} It may be a result of aggregation and possible denaturation

from high local protein concentration, as well as an artifact of freeze–thawing of samples rendering some fraction of the release samples undetectable by ELISA. The apparent reduction in released quantities of proteins from this affinity system due to sample freezing and thawing has been observed before and is much more significant in release samples with low protein concentration, such as those from HAMC-SBP after 24 h.^{7,73}

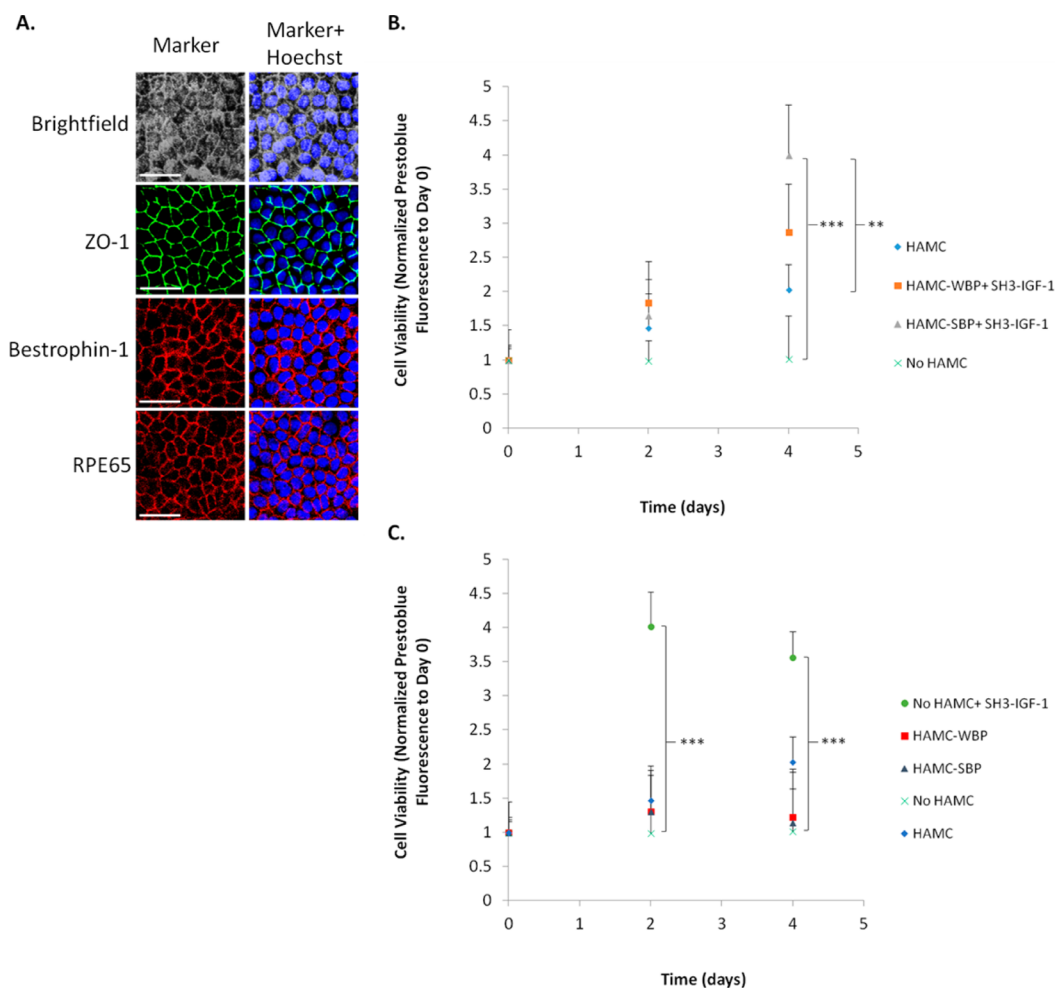


Figure 6. (A) RPEs derived from hES cells exhibited typical RPE morphology, were pigmented, and uniformly expressed the tight junction marker ZO-1 and the RPE markers Bestrophin-1 and RPE65. The scale bar is 30 μm . (B) HAMC-SBP with SH3-IGF-1 significantly increased the proliferation of RPEs *in vitro* at day 4 relative to that with HAMC ($p < 0.01$) and SFM (no HAMC, $p < 0.001$). RPEs were suspended in serum-free DMEM/F-12 or encapsulated in (0.75%/0.75% (w/v)) HAMC, HAMC-WBP with 10 $\mu\text{g}/\text{mL}$ SH3-IGF-1 (270:1 molar ratio WBP/SH3-IGF-1), or HAMC-SBP with 10 $\mu\text{g}/\text{mL}$ SH3-IGF-1 (50:1 molar ratio SBP/SH3-IGF-1) hydrogels. (C) SH3-IGF-1 alone significantly increased the proliferation of RPEs *in vitro*. RPEs were suspended in serum-free DMEM/F-12 with or without 10 $\mu\text{g}/\text{mL}$ SH3-IGF-1 or encapsulated in HAMC, HAMC-WBP, or HAMC-SBP. The cells were plated on poly(HEMA)-coated nonadhesive 96-well plates and incubated for 0, 2, and 4 days. Cell viability was measured by the Prestobluo metabolic assay. RPEs in serum-free media with SH3-IGF-1 showed significantly increased viability compared to that of RPEs in serum-free media alone ($p < 0.001$) at days 2 and 4 ($n = 6$ for HAMC and no HAMC conditions; $n = 3$ for all other conditions; mean + standard deviation plotted; ** $p < 0.01$ and *** $p < 0.001$, one-way ANOVA, Tukey's *post hoc* test).

This phenomenon can potentially disguise a slow release rate, giving the appearance of a plateau.

RPEs, derived from human embryonic stem (hES) cells, were pigmented and exhibited typical morphology and marker expression (Figure 6A), in agreement with what has been reported by others.⁷⁴ RPE viability in HAMC gels was then tested on nonadhesive poly(HEMA)-coated plates. RPEs encapsulated in HAMC-SBP/SH3-IGF-1 showed increased viability at day 4 in comparison to RPEs in HAMC alone ($p < 0.01$) or serum-free media (SFM) ($p < 0.001$; Figure 6B). Interestingly, the addition of soluble SH3-IGF-1 to SFM led to increased RPE viability on days 2 and 4 ($p < 0.001$) compared to that with SFM alone (Figure 6C). Cells under all conditions either maintained or experienced decreased viability after day 4, possibly due to depleted nutrients in the same SFM. There were no significant differences in viability between RPEs in HAMC-SBP and HAMC-WBP with or without SH3-IGF-1 at any time point ($p > 0.05$; Figure 6AB). In addition, RPEs in HAMC exhibited similar survival to that of RPEs in HAMC-

WBP or HAMC-SBP in the absence of SH3-IGF-1 ($p > 0.05$; Figure 6B).

Despite, or possibly because of, the plateau phenomenon in HAMC-SBP gels, these hydrogels demonstrated the most potent effects on RPE viability, with 2- and 4-fold greater cell viability than that of cells in HAMC alone or SFM alone, respectively, based on the Prestobluo signal. When SFM was supplemented with SH3-IGF-1, the 4-fold increase in RPE survival was observed on day 1, which is earlier than that in the HAMC-SBP/SH3-IGF-1 hydrogels, and maintained until day 4. This could indicate increased availability of IGF-1 in SFM at the earlier time points compared to that with HAMC-SBP, potentially because of the delayed release of IGF-1 in the gels. RPE viability in the HAMC-WBP/SH3-IGF-1 gels was significantly (3-fold) greater than that with SFM alone; however, it was not statistically different from that with HAMC alone. This may be attributed to the quicker release of SH3-IGF-1 from HAMC-WBP, from the gels into the media, where it becomes unavailable to the cells. Thus, the tunable,

controlled-release IGF-1 hydrogel is coupled with RPE cell viability under anchorage-independent conditions.

To confirm that the effects of RPE proliferation can indeed be attributed to SH3–IGF-1, we ran a series of controls (Figure 6C), where only SFM supplemented with SH3–IGF-1 had a 4-fold increase in RPE survival on days 2 and 4. None of the other vehicle controls, where SH3–IGF-1 was absent, showed any cell proliferation. This series of controls was important, as HAMC itself can promote cell survival and proliferation.^{75–77} The CD44 receptor, which binds to HA and promotes cell survival,⁷⁸ is upregulated in proliferating RPEs.⁷⁹ The proliferative effects of IGF-1 on RPEs may increase the prosurvival and proliferative effects of CD44 on RPEs, increasing the beneficial effects of the material. However, since we did not observe a significant difference in survival between RPEs in HAMC alone and SFM conditions, we attribute the difference in the number of viable cells to IGF-1. We acknowledge that our hES-derived RPEs are more representative of fetal human RPEs rather than primary adult human RPEs. The latter may respond differently to our gels and/or IGF-1.

4. CONCLUSIONS

HAMC hydrogels modified with SH3-binding peptides were able to attenuate the release of SH3–IGF-1 fusion protein over several days in comparison to that with HAMC gels alone. The rate of release of SH3–IGF-1 is slower from HAMC-SBP gels than from HAMC-WBP gels, thereby reflecting the difference in equilibrium binding between the strong and weak binding peptides and SH3. This system was able to release a greater proportion of IGF-1 than other IGF-1 affinity systems on a similar time scale. Encapsulation of RPEs within the HAMC-IGF-1 release system was shown to increase cell viability under anchorage-independent conditions *in vitro* in comparison to that with serum-free media or HAMC alone. This work shows that tunable protein delivery improves cell viability and that IGF-1 promotes RPE cell viability under anchorage-independent conditions. This new type of multifunctional material is efficacious *in vitro* to simultaneously extend the benefit of protein therapeutics on cells through sustained delivery while increasing the viability of encapsulated cells via interactions with the biomaterial and localized biomolecule. This system lays the foundation for future *in vivo* studies where we anticipate that this combined cell and biomolecule delivery system will enhance cell survival after transplantation, thereby overcoming one of the key barriers to success.

■ ASSOCIATED CONTENT

Supporting Information

The Supporting Information is available free of charge on the ACS Publications website at DOI: 10.1021/acs.biomac.5b01366.

Gel electrophoresis pictures of the synthesis, expression, and purification of SH3–IGF-1 (Figure S1); mass spectrometry plot demonstrating the purity of the protein (Figure S2) (PDF)

■ AUTHOR INFORMATION

Corresponding Author

*E-mail: molly.shoichet@utoronto.ca.

Author Contributions

[†]J.P. and N.M. contributed equally to this work.

Notes

The authors declare no competing financial interest.

■ ACKNOWLEDGMENTS

This research was supported by the Natural Sciences and Engineering Research Council (Discovery Grant to M.S.S., CGS-M to J.P., and NSERC CREATE in M3 scholarship to N.M.). We are grateful to Dr. Karen Maxwell (University of Toronto) and members of her lab for the modified pET32b vector, Dr. Andras Nagy (University of Toronto) for the CA1 hES line, and members of the Shoichet lab for their thoughtful discussions.

■ REFERENCES

- (1) Schmeer, C. W.; Wohl, S. G.; Isenmann, S. Cell-replacement therapy and neural repair in the retina. *Cell Tissue Res.* **2012**, *349* (1), 363–374.
- (2) Sheffield, W. P. Modification of clearance of therapeutic and potentially therapeutic proteins. *Curr. Drug Targets: Cardiovasc. & Haematol. Disord.* **2001**, *1* (1), 1–22.
- (3) El Sanharawi, M.; Kowalczyk, L.; Touchard, E.; Omri, S.; de Kozak, Y.; Behar-Cohen, F. Protein delivery for retinal diseases: From basic considerations to clinical applications. *Prog. Retinal Eye Res.* **2010**, *29* (6), 443–465.
- (4) Sivasubramanian, M.; Thambi, T.; Park, J. H. Mineralized cyclodextrin nanoparticles for sustained protein delivery. *Carbohydr. Polym.* **2013**, *97* (2), 643–649.
- (5) Vulic, K.; Shoichet, M. S. Affinity-based drug delivery systems for tissue repair and regeneration. *Biomacromolecules* **2014**, *15* (11), 3867–3880.
- (6) Putney, S.; Burke, P. Improving protein therapeutics with sustained-release formulations. *Nat. Biotechnol.* **1998**, *16* (2), 153–157.
- (7) Vulic, K.; Shoichet, M. S. Tunable growth factor delivery from injectable hydrogels for tissue engineering. *J. Am. Chem. Soc.* **2012**, *134* (2), 882–885.
- (8) Rao, K.; El-Hami, K.; Kodaki, T.; Matsushige, K.; Makino, K. A novel method for synthesis of silica nanoparticles. *J. Colloid Interface Sci.* **2005**, *289* (1), 125–131.
- (9) Yang, H.; Tyagi, P.; Kadam, R. S.; Holden, C. A.; Kompella, U. B. Hybrid dendrimer hydrogel/PLGA nanoparticle platform sustains drug delivery for one week and antiglaucoma effects for four days following one-time topical administration. *ACS Nano* **2012**, *6* (9), 7595–7606.
- (10) Lu, Y.; Zhou, N.; Huang, X.; et al. Effect of intravitreal injection of bevacizumab-chitosan nanoparticles on retina of diabetic rats. *Int. J. Ophthalmol.* **2014**, *7* (1), 1–7.
- (11) Akiyama, G.; Sakai, T.; Kuno, N.; et al. Photoreceptor rescue of pigment epithelium-derived factor-impregnated nanoparticles in royal college of surgeons rats. *Mol. Vis.* **2012**, *18* (314–15), 3079–3086.
- (12) Fu, K.; Klibanov, A. M.; Langer, R. Protein stability in controlled-release systems. *Nat. Biotechnol.* **2000**, *18* (1), 24–25.
- (13) Colletier, J.; Chaize, B.; Winterhalter, M.; Fournier, D. Protein encapsulation in liposomes: Efficiency depends on interactions between protein and phospholipid bilayer. *BMC Biotechnol.* **2002**, *2* (1), 9.
- (14) Pakulska, M. M.; Vulic, K.; Shoichet, M. S. Affinity-based release of chondroitinase ABC from a modified methylcellulose hydrogel. *J. Controlled Release* **2013**, *171* (1), 11–16.
- (15) Vulic, K.; Shoichet, M. S. Affinity-based drug delivery systems for tissue repair and regeneration. *Biomacromolecules* **2014**, *15* (11), 3867–3880.
- (16) Jeon, O.; Kang, S.; Lim, H.; Chung, J.; Kim, B. Long-term and zero-order release of basic fibroblast growth factor from heparin-conjugated poly(L-lactide-co-glycolide) nanospheres and fibrin gel. *Biomaterials* **2006**, *27* (8), 1598–1607.
- (17) Ruvinov, E.; Leor, J.; Cohen, S. The promotion of myocardial repair by the sequential delivery of IGF-1 and HGF from an injectable

alginate biomaterial in a model of acute myocardial infarction. *Biomaterials* **2011**, *32* (2), 565–578.

(18) Tam, R. Y.; Fuehrmann, T.; Mitrousis, N.; Shoichet, M. S. Regenerative therapies for central nervous system diseases: A biomaterials approach. *Neuropsychopharmacology* **2014**, *39* (1), 169–188.

(19) Kaplan, H. J.; Tezel, T. H.; Berger, A. S.; Del Priore, L. V. Retinal transplantation. In *Immune Response and the Eye*; Streilein, J. W., Ed.; Karger: Basel, 1999; pp 207–219.

(20) Lester, L. B.; Francis-Pau, K. Y.; Wolf, D. P. Preclinical trials for stem cell therapy. In *Stem Cells in Endocrinology*; Lester, L. B., Ed.; Humana Press: Totowa, NJ, 2007; p 250.

(21) Schwartz, S. D.; Hubschman, J.; Heilwell, G.; et al. Embryonic stem cell trials for macular degeneration: A preliminary report. *Lancet* **2012**, *379* (9817), 713–720.

(22) Ding, X.; Patel, M.; Chan, C. Molecular pathology of age-related macular degeneration. *Prog. Retinal Eye Res.* **2009**, *28* (1), 1–18.

(23) Strauss, O. The role of retinal pigment epithelium in visual functions. *Ophthalmology* **2009**, *106* (4), 299–304.

(24) Afshari, F. T.; Fawcett, J. W. Improving RPE adhesion to bruch's membrane. *Eye* **2009**, *23* (10), 1890–1893.

(25) Pan, C. K.; Heilwell, G.; Lanza, R.; Schwartz, S. D. Embryonic stem cells as a treatment for macular degeneration. *Expert Opin. Biol. Ther.* **2013**, *13* (8), 1125–1133.

(26) Afshari, F. T.; Kwok, J. C.; Andrews, M. R.; et al. Integrin activation or alpha9 expression allows retinal pigmented epithelial cell adhesion on bruch's membrane in wet age-related macular degeneration. *Brain* **2010**, *133*, 448–464.

(27) Heller, J. P.; Martin, K. R. Enhancing RPE cell-based therapy outcomes for AMD: The role of bruch's membrane. *Transl. Vis. Sci. Technol.* **2014**, *3* (4), 4.

(28) Sakai, S.; Liu, Y.; Sengoku, M.; Taya, M. Cell-selective encapsulation in hydrogel sheaths via biospecific identification and biochemical cross-linking. *Biomaterials* **2015**, *53*, 494–501.

(29) Burdick, J.; Anseth, K. Photoencapsulation of osteoblasts in injectable RGD-modified PEG hydrogels for bone tissue engineering. *Biomaterials* **2002**, *23* (22), 4315–4323.

(30) Burdick, J. A.; Prestwich, G. D. Hyaluronic acid hydrogels for biomedical applications. *Adv. Mater.* **2011**, *23* (12), H41–H56.

(31) Mothe, A. J.; Tam, R. Y.; Zahir, T.; Tator, C. H.; Shoichet, M. S. Repair of the injured spinal cord by transplantation of neural stem cells in a hyaluronan-based hydrogel. *Biomaterials* **2013**, *34* (15), 3775–3783.

(32) Tam, R. Y.; Cooke, M. J.; Shoichet, M. S. A covalently modified hydrogel blend of hyaluronan-methyl cellulose with peptides and growth factors influences neural stem/progenitor cell fate. *J. Mater. Chem.* **2012**, *22*, 19402–19411.

(33) Baumann, M. D.; Kang, C. E.; Tator, C. H.; Shoichet, M. S. Intrathecal delivery of a polymeric nanocomposite hydrogel after spinal cord injury. *Biomaterials* **2010**, *31* (30), 7631–7639.

(34) Gupta, D.; Tator, C. H.; Shoichet, M. S. Fast-gelling injectable blend of hyaluronan and methylcellulose for intrathecal, localized delivery to the injured spinal cord. *Biomaterials* **2006**, *27* (11), 2370–2379.

(35) Shoichet, M. S.; Tator, C. H.; Poon, P.; Kang, K.; Baumann, M. D. Intrathecal drug delivery strategy is safe and efficacious for localized delivery to the spinal cord. *Prog. Brain Res.* **2007**, *161*, 385–92.

(36) Ballios, B. G.; Cooke, M. J.; van der Kooy, D.; Shoichet, M. S. A hydrogel-based stem cell delivery system to treat retinal degenerative diseases. *Biomaterials* **2010**, *31* (9), 2555–2564.

(37) Ballios, B.; Cooke, M.; Donaldson, L. A hyaluronan-based injectable hydrogel improves the survival and integration of stem cell progeny following transplantation. *Stem Cell Rep.* **2015**, *4* (6), 1031–1045.

(38) Beriat, G. K.; Akmansu, S. H.; Dogan, C.; et al. The effect of subcutaneous insulin-like growth factor-1 (IGF-1) injection on rabbit auricular cartilage autograft viability. *Bosnian J. Basic Med. Sci.* **2012**, *12* (4), 213–218.

(39) Dai, W.; Kloner, R. A. Cardioprotection of insulin-like growth factor-1 during reperfusion therapy what is the underlying mechanism or mechanisms? *Circ.: Cardiovasc. Interventions* **2011**, *4* (4), 311–313.

(40) Seigel, G.; Chiu, L.; Paxhia, A. Inhibition of neuroretinal cell death by insulin-like growth factor-1 and its analogs. *Mol. Vis.* **2000**, *6* (19), 157–163.

(41) Seigel, G. M.; Lupien, S. B.; Campbell, L. A.; Ishii, D. N. Systemic IGF-I treatment inhibits cell death in diabetic rat retina. *J. Diabetes Complications* **2006**, *20* (3), 196–204.

(42) ZAPP, J.; FROESCH, E. Insulin-like growth-factors somatomedins - structure, secretion, biological actions and physiological-role. *Horm. Res.* **1986**, *24* (2–3), 121–130.

(43) Sherrard, R.; Bower, A. Role of afferents in the development and cell survival of the vertebrate nervous system. *Clin. Exp. Pharmacol. Physiol.* **1998**, *25* (7–8), 487–495.

(44) Valenciano, A. I.; Boya, P.; de la Rosa, E. J. Early neural cell death: Numbers and cues from the developing neuroretina. *Int. J. Dev. Biol.* **2009**, *53* (8–10), 1515–1528.

(45) West, E. L.; Pearson, R. A.; Duran, Y.; et al. Manipulation of the recipient retinal environment by ectopic expression of neurotrophic growth factors can improve transplanted photoreceptor integration and survival. *Cell Transplant.* **2012**, *21* (5), 871–887.

(46) GRANT, M.; GUAY, C.; MARSH, R. Insulin-like growth factor-1 stimulates proliferation, migration, and plasminogen-activator release by human retinal-pigment epithelial-cells. *Curr. Eye Res.* **1990**, *9* (4), 323–335.

(47) Peruzzi, F.; Prisco, M.; Dews, M.; et al. Multiple signaling pathways of the insulin-like growth factor 1 receptor in protection from apoptosis. *Mol. Cell. Biol.* **1999**, *19* (10), 7203–7215.

(48) Parrizas, M.; Saltiel, A.; LeRoith, D. Insulin-like growth factor 1 inhibits apoptosis using the phosphatidylinositol 3'-kinase and mitogen-activated protein kinase pathways. *J. Biol. Chem.* **1997**, *272* (1), 154–161.

(49) Wang, H.; Liao, S.; Geng, R. IGF-1 signaling via the PI3K/akt pathway confers neuroprotection in human retinal pigment epithelial cells exposed to sodium nitroprusside insult. *J. Mol. Neurosci.* **2015**, *55*, 931–940.

(50) Weng, C. Y.; Kothary, P. C.; Verkade, A. J.; Reed, D. M.; Del Monte, M. A. MAP kinase pathway is involved in IGF-1-stimulated proliferation of human retinal pigment epithelial cells (hRPE). *Curr. Eye Res.* **2009**, *34* (10), 867–876.

(51) Chaum, E.; Yang, H. T. Transgenic expression of IGF-1 modifies the proliferative potential of human retinal pigment epithelial cells. *Invest. Ophthalmol. Vis. Sci.* **2002**, *43* (12), 3758–3764.

(52) Barazi, H. O.; Zhou, L. G.; Templeton, N. S.; Krutzsch, H. C.; Roberts, D. D. Identification of heat shock protein 60 as a molecular mediator of alpha 3 beta 1 integrin activation. *Cancer Res.* **2002**, *62* (5), 1541–1548.

(53) Salani, B.; Briatore, L.; Contini, P.; et al. IGF-I induced rapid recruitment of integrin beta(1) to lipid rafts is caveolin-1 dependent. *Biochem. Biophys. Res. Commun.* **2009**, *380* (3), 489–492.

(54) Saegusa, J.; Yamaji, S.; Ieguchi, K.; et al. The direct binding of insulin-like growth factor-1 (IGF-1) to integrin alpha v beta 3 is involved in IGF-1 signaling. *J. Biol. Chem.* **2009**, *284* (36), 24106–24114.

(55) Fujita, M.; Ieguchi, K.; Davari, P.; et al. Cross-talk between integrin alpha 6 beta 4 and insulin-like growth factor-1 receptor (IGF1R) through direct alpha 6 beta 4 binding to IGF1 and subsequent alpha 6 beta 4-IGF1-IGF1R ternary complex formation in anchorage-independent conditions. *J. Biol. Chem.* **2012**, *287* (15), 12491–12500.

(56) Alfano, D.; Iaccarino, I.; Stoppelli, M. P. Urokinase signaling through its receptor protects against anoikis by increasing BCL-xL expression levels. *J. Biol. Chem.* **2006**, *281* (26), 17758–17767.

(57) Khwaja, A.; Rodriguez-Viciano, P.; Wennstrom, S.; Warne, P. H.; Downward, J. Matrix adhesion and ras transformation both activate a phosphoinositide 3-OH kinase and protein kinase B/akt cellular survival pathway. *EMBO J.* **1997**, *16* (10), 2783–2793.

- (58) Porstmann, T.; Griffiths, B.; Chung, Y. L.; et al. PKB/akt induces transcription of enzymes involved in cholesterol and fatty acid biosynthesis via activation of SREBP. *Oncogene* **2005**, *24* (43), 6465–6481.
- (59) Uebersax, E. D.; Grindstaff, R. D.; Defoe, D. M. Survival of the retinal pigment epithelium in vitro: Comparison of freshly isolated and subcultured cells. *Exp. Eye Res.* **2000**, *70* (3), 381–390.
- (60) Han, S.; Ham, T. R.; Haque, S.; Sparks, J. L.; Saul, J. M. Alkylation of human hair keratin for tunable hydrogel erosion and drug delivery in tissue engineering applications. *Acta Biomater.* **2015**, *23*, 201–213.
- (61) Balcom, N. T.; Berg-Johansen, B.; Dills, K. J.; et al. In vitro articular cartilage growth with sequential application of IGF-1 and TGF-beta 1 enhances volumetric growth and maintains compressive properties. *J. Biomech. Eng.* **2012**, *134* (3), 031001.
- (62) Florine, E. M.; Miller, R. E.; Liebesny, P. H.; et al. Delivering heparin-binding insulin-like growth factor 1 with self-assembling peptide hydrogels. *Tissue Eng., Part A* **2015**, *21* (3–4), 637–646.
- (63) Ma, J.; Guo, C.; Guo, C.; et al. Transplantation of human neural progenitor cells expressing IGF-1 enhances retinal ganglion cell survival. *PLoS One* **2015**, *10* (4), e0125695.
- (64) Kang, C. E.; Poon, P. C.; Tator, C. H.; Shoichet, M. S. A new paradigm for local and sustained release of therapeutic molecules to the injured spinal cord for neuroprotection and tissue repair. *Tissue Eng., Part A* **2009**, *15* (3), 595–604.
- (65) Phung, Y. T.; Barbone, D.; Broaddus, V. C.; Ho, M. Rapid generation of in vitro multicellular spheroids for the study of monoclonal antibody therapy. *J. Cancer* **2011**, *2*, 507–514.
- (66) Klimanskaya, I.; Hipp, J.; Rezai, K.; West, M.; Atala, A.; Lanza, R. Derivation and comparative assessment of retinal pigment epithelium from human embryonic stem cells using transcriptomics. *Cloning Stem Cells* **2004**, *6* (3), 217–245.
- (67) D'Esposito, V.; Passaretti, F.; Hammarstedt, A.; et al. Adipocyte-released insulin-like growth factor-1 is regulated by glucose and fatty acids and controls breast cancer cell growth in vitro. *Diabetologia* **2012**, *55* (10), 2811–2822.
- (68) Pacher, M.; Seewald, M. J.; Mikula, M.; et al. Impact of constitutive IGF1/IGF2 stimulation on the transcriptional program of human breast cancer cells. *Carcinogenesis* **2007**, *28* (1), 49–59.
- (69) Ritger, P. L.; Peppas, N. A. A simple equation for description of solute release I. fickian and non-fickian release from non-swelling devices in the form of slabs, spheres, cylinders or discs. *J. Controlled Release* **1987**, *5* (1), 23–36.
- (70) Willerth, S. M.; Johnson, P. J.; Maxwell, D. J.; Parsons, S. R.; Doukas, M. E.; Sakiyama-Elbert, S. E. Rationally designed peptides for controlled release of nerve growth factor from fibrin matrices. *J. Biomed. Mater. Res., Part A* **2007**, *80A* (1), 13–23.
- (71) Jha, A. K.; Mathur, A.; Svedlund, F. L.; Ye, J.; Yeghiazarians, Y.; Healy, K. E. Molecular weight and concentration of heparin in hyaluronic acid-based matrices modulates growth factor retention kinetics and stem cell fate. *J. Controlled Release* **2015**, *209*, 308–316.
- (72) Joung, Y. K.; Bae, J. W.; Park, K. D. Controlled release of heparin-binding growth factors using heparin-containing particulate systems for tissue regeneration. *Expert Opin. Drug Delivery* **2008**, *5* (11), 1173–1184.
- (73) Vulic, K.; Pakulska, M. M.; Sonthalia, R.; Ramachandran, A.; Shoichet, M. S. Mathematical model accurately predicts protein release from an affinity-based delivery system. *J. Controlled Release* **2015**, *197*, 69–77.
- (74) Vugler, A.; Carr, A.; Lawrence, J.; et al. Elucidating the phenomenon of HESC-derived RPE: Anatomy of cell genesis, expansion and retinal transplantation. *Exp. Neurol.* **2008**, *214* (2), 347–361.
- (75) Trochon, V.; Mabilat, C.; Bertrand, P.; et al. Evidence of involvement of CD44 in endothelial cell proliferation, migration and angiogenesis in vitro. *Int. J. Cancer* **1996**, *66* (5), 664–668.
- (76) Tsuneki, M.; Madri, J. A. CD44 regulation of endothelial cell proliferation and apoptosis via modulation of CD31 and VE-cadherin expression. *J. Biol. Chem.* **2014**, *289* (9), 5357–5370.
- (77) Stamenkovic, I.; Yu, Q. Merlin, a “magic” linker between the extracellular cues and intracellular signaling pathways that regulate cell motility, proliferation, and survival. *Curr. Protein Pept. Sci.* **2010**, *11* (6), 471–484.
- (78) Bunek, J.; Kamarajan, P.; Kapila, Y. L. Anoikis mediators in oral squamous cell carcinoma. *Oral Dis.* **2011**, *17* (4), 355–361.
- (79) Liu, N. P.; Roberts, W. L.; Hale, L. P.; et al. Expression of CD44 and variant isoforms in cultured human retinal pigment epithelial cells. *Invest. Ophthalmol. Vis. Sci.* **1997**, *38* (10), 2027–2037.